Smart Structures and Systems, *Vol. 22, No. 6 (2018) 675-687*
DOI: https://doi.org/10.12989/sss.2018.22.6.675

Simulation of fracture mechanism of pre-holed concrete model under Brazilian test using PFC3D

Vahab Sarfarazi[1], Hadi Haeri*[2] and Alireza Bagher Shemirani[3]

[1]*Department of Mining Engineering, Hamedan University of Technology, Hamedan, Iran*
[2]*Young Researchers and Elite Club, Bafgh Branch, Islamic Azad University, Bafgh, Iran*
[3]*Department of Civil Engineering, Sadra Institute of Higher Education, Tehran, Iran*

(Received August 23, 2018, Revised November 14, 2018, Accepted November 16, 2018)

Abstract. In the previous studies on the porous rock strength the effect of pore number and its diameter is not explicitly defined. In this paper crack initiation, propagation and coalescence in Brazilian model disc containing a single cylindrical hole and or multiple holes have been studied numerically using PFC3D. In model with internal hole, the ratio of hole diameter to model diameter was varied between 0.03, 0.17, 0.25, 0.33, and 0.42. In model with multiple hole number of holes was different in various model, i.e., one hole, two holes, three holes, four holes, five holes, six holes, seven holes, eight holes and nine holes. Diameter of these holes was 5 mm, 10 mm and 12 mm. The pre-holed Brazilian discs are numerically tested under Brazilian test. The breakage load in the ring type disc specimens containing an internal hole with varying diameters is measured. The mechanism of cracks propagation in the wall of the ring type specimens is also studied. In the case of multi-hole Brazilian disc, the cracks propagation and b cracks coalescence are also investigated. The results shows that breaking of the pre-holed disc specimens is due to the propagation of radially induced tensile cracks initiated from the surface of the central hole and propagating toward the direction of diametrical loading. In the case of disc specimens with multiple holes, the cracks propagation and cracks coalescence may occur simultaneously in the breaking process of model under diametrical compressive loading. Finally the results shows that the failure stress and crack initiation stress decreases by increasing the hole diameter. Also, the failure stress decreases by increasing the number of hole which mobilized in failure. The results of these simulations were comprised with other experimental and numerical test results. It has been shown that the numerical and experimental results are in good agreement with each other.

Keywords: concrete rings; pre-holed Brazilian disc; crack analyses; coalescence; PFC3D

1. Introduction

The cracks initiation, propagation and coalescence can control the failure of concretes. These cracks usually emanate from the natural pores or pre-existing cracks with in the concrete structures under different practically applied loading conditions, Therefore, some theoretical, experimental and numerical studies have been accomplished on the mechanism of the crack growth and extension in material specimens containing pores and multiple cracks in the literature (Lajtai 1975, Robert *et al*. 1979, Nemat-Nasser *et al.* 1982, Sammis 1986, Ashby *et al.* 1986, Wong 1998, Lin 2005, Park 2009, Jespersen 2010, Lancaster *et al*. 2013, Ramadoss 2013, Pan *et al*. 2014, Mobasher *et al.* 2014, Noel and Soudki 2014, Oliveira and Leonel 2014, Tiang *et al*. 2015, Wan Ibrahim *et al.* 2015, Silva *et al.* 2015, Gerges *et al*. 2015, Liu *et al*. 2015, Lin 2015, Lee and Chang 2015, Kequan and Zhoudao 2015, Fan *et al.* 2016, Li *et al*. 2015, 2016, Yaylac 2016, Sardemir 2016, Shuraim 2016, Akbas 2016, Haeri *et al.* 2016a, b, c, Haeri and Sarfarazi 2016, Rajabi 2016, Mohammad 2016, Wang *et al.* 2017). The previous results show that an analysis of the stress distribution around a crack indicates the points of fracture initiation as well as the initial direction of crack propagation. As a result of the change in stress distribution associated with fracture propagation it is, however, impossible to predict the final path of the propagating crack. Consequently, a serious limitation of the Griffith theory lies in the fact that it can only be used to predict fracture initiation. In its usual form, it yields no information on the rate or direction of fracture propagation. The earlier studies have shown that two kinds of cracks, e.g., wing cracks and secondary cracks, may initiate from the tip of a single open crack under uniaxial compression. Wing cracks are induced by the tensile force, while secondary cracks are the result of shear force. In the loading process, wing cracks appear earlier than secondary cracks. The secondary cracks make the failure of the whole specimen. Lajtai (1975), tensile wing cracks were found to first appear at the tips of horizontal joints, followed by the secondary shear cracks propagating towards the opposite joint. Wong 1998, represent that under internal or external pressures, pre-existing defects can induce macro crack, which can in turn change the structure of the rock.

Sardemir (2016) represent that presence of natural weaknesses around the crack tip could change the stress distribution around the crack tip and lead to variations of characteristics of crack tip plastic zone

*Corresponding author, Assistant Professor
E-mail: h.haeri@bafgh-iau.ac.ir; haerihadi@gmail.com

ISSN: 1738-1584 (Print), 1738-1991 (Online)

such as plastic zone size and plastic zone shape. Such micro defects affect the fracture toughness and extension or kinking of the macro crack. Robert *et al.* (1979) represent that when cracks are analyzed, the behavior of the material ahead of the crack tip is considered isotropic, i.e., plastic deformation occurs identically in all directions and there are no preferred directions for the plastic deformation. In this case, the plastic deformation can be mathematically formulated with the help of classical isotropic plasticity. This situation significantly differs when the crack tip is near a micro-defect; the plastic zone ahead of the crack tip will be affected by the presence of the micro-defects.

Theoretically, linear elastic stress analysis of cracks predicts infinite stresses at the crack tip. In fact, inelastic deformation, such as plasticity in ductile and brittle materials, leads to relaxation of crack tip stresses caused by the yielding phenomenon at the crack tip (Nemat-Nasser *et al.* 1982).

Jespersen (2010) represent that most rock materials develop plastic strains when the yield strength is exceeded in the region near a crack tip. Thus, the amount of plastic deformation is restricted by the surrounding material, which remains elastic during loading. The formation of the plastic zone in a homogeneous material depends on the material properties, structural element configuration, and loading conditions. The size of the plastic zone can be estimated when moderate crack tip yielding occurs.

A set of uniaxial compression tests were carried out on plate type specimens containing a single hole or array of holes with the same size or with different sizes by Sammis and Ashby (1986). They experimentally investigated the cracks coalescence phenomena in the propagating cracks and also their interaction with the surfaces of the specimens. The Central Straight through Crack Brazilian Disc (CSCBD) specimens of brittle limestone was used by Al-Shayea (2005), to accomplish some experimental studies on the crack extensions paths in these rock samples. He considered the effects of different crack inclination angles on the cracks propagating pattern of lime stone samples under the mixed Mode I/II loading conditions. Mellor and Hawkes (1971) experimentally studied the cracks propagation mechanism in ring type specimens under diametrical compression loading. The cracks coalescence and interaction mechanism in granite rock samples containing multiple holes were also investigated by Lin *et al.* (2015).

On the other hand, many numerically simulation approaches such as finite element method (FEM), boundary element method (BEM) and finite difference method (FDM) have been developed to study the cracks initiations, cracks propagations and cracks coalescences mechanism in various brittle materials such as rocks, concretes and ceramics. For example the finite element method have been carried out by Roy (1999), Sukumar (2003), Lin (2014), the boundary element method by Altiero (1982), Aliabadi (1993), Haeri *et al*. (2015a, b, c), and the finite difference method (Cundall 1979, Ghazvinian 2012, Sarfarazi 2014). Some other specially developed sophisticated numerical methods for cracks analyses in brittle materials include the discontinuous deformation analysis (Shi 1988, Zheng 2009, Amadei 1996), discrete numerical modelling, (Cundall 1979, Ghazvinian 2012, Lin 2013, Sarfarazi 2014), 3D numerical manifold method (He 2010) and the displacement discontinuity method (Crouch 1976, Fatehi Marji 1989, Tan 1998, Fatehi Marji *et al.* 2014). However, in the present work, the three dimensional particle flow code (PFC3D) which is based on the sophisticated discrete element method (DEM) is used to simulate the crack propagation mechanism in the modelled disc type specimens containing single hole or multiple holes under compressive loading condition. The failure process and the fracturing patterns including the cracks initiation and cracks extension and cracks coalescence and their interactions with the specimen's boundary are being studied for the disc models containing cylindrical holes with different sizes. The effects of the bridge area (i.e., the area in between the two neighboring holes) and also the effects of the number of holes on the crack propagation patterns and failure mechanism of the modeled discs are numerically investigated.

2 Three dimensional particle flow code (PFC3D) using the bonded particle model

To simulate a rock sample in PFC3D, it is required to present the rock material as an assembly of bonded disc type particles which are rigid but can move relative to one another and are in contact with each other at the contact points. These particle assemblies are confined by walls to model a typical rock sample. However, two types of bonding models are being adopted in PFC3D which are: i) the contact bond model and ii) the parallel bond model. In the contact bond model, the physical behavior of the small cement like material lying in between the two adjacent bonded particles is approximately determined. The contact bond model corresponds to a parallel bond model with a radius of zero it means that the contact model unlike that of the parallel bond does not have a radius therefore, have no normal or shear stiffness's so that it cannot resist the bending moment but can only resist the forces acting at the contact points with in a particle assembly. On the other hand, the parallel bonds are adopted specified tensile and shear strengths values which them to resist the tensile and shear forces at the contacts until the contact forces exceed the corresponding strengths of the bonds. Cundall (1979) proposed an approach to generate a parallel bond model for PFC3D. in this modeling approach, the following micro parameters are suggested for modelling a particular particle assembly: the stiffness ratio, Kn (normal stiffness) over Ks (shear stiffness), the contact modulus for ball to ball, the normal and shear bonding strengths at the contacts, the ratio of the strengths' standard deviation to that of the normal and shear bonding strengths, the minimum ball radius. In addition to these parameters, three micro parameters are also required for the modeling for a parallel-bonding particle model including the multiplier for the parallel-bond radius, the modulus and the stiffness ratio for the parallel-bond.

Table 1 Micro properties used to represent the intact rock

Parameter	Value	Parameter	Value
Type of particle	disc	Parallel bond radius multiplier	1
Density (kg/m^3)	3000	Young Modulus of parallel bond (GPa)	40
Minimum radius (mm)	0.27	Parallel bond stiffness ratio	1.7
Size ratio	1.56	Particle friction coefficient	0.4
Porosity ratio	0.08	Parallel bond normal strength, mean (MPa)	7
Damping coefficient	0.7	Parallel bond normal strength, SD (MPa)	2
Contact young modulus (GPa)	40	Parallel bond shear strength, mean (MPa)	7
Stiffness ratio	1.7	Parallel bond shear strength, SD (MPa)	2

Table 2 Brazilian tensile strength of physical and numerical samples

Physical tensile strength (MPa)	1.5 and 1.7
Numerical tensile strength (MPa)	1.5

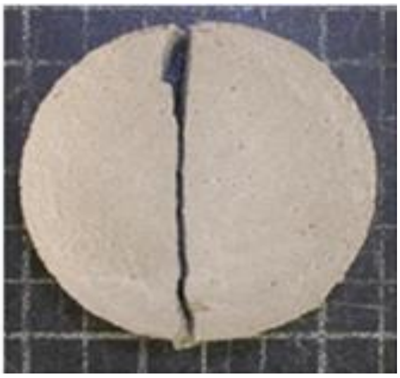

(a)

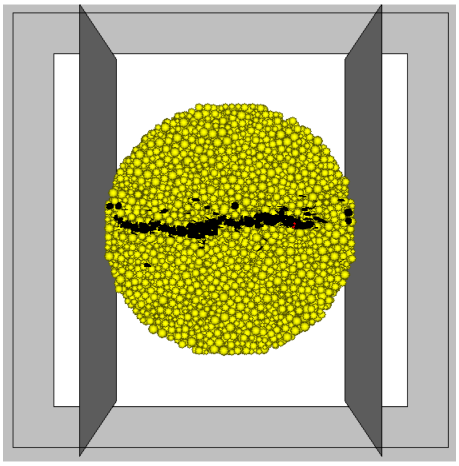

(b)

Fig. 1 Failure pattern in (a) physical sample and (b) PFC3D model

2.1 Numerical model's preparation and calibration procedures

The standard indirect Brazilian tensile testing procedure is used for calibrating the tensile strength of the material specimen modeled in PFC3D as a particular particle assembly. The test model can be generated by a standard process involving four steps: i) generation and packing of the particles in the assembly, ii) the installation of isotropic stress state, ii) the elimination of floating particles and iv) the installation of particle bonding. The standard calibration procedure suggested by Ghazvinian (2012) is adopted using the micro properties listed in Table 1 to calibrate the Brazilian disc type samples simulated in PFC3D as a particular assembly. The dimension of this particle assembly is 54 mm and a total number of 5,615 particles are generated. A standard low speed of 0.016 m/s is used to crush the lateral walls of the modelled specimen toward each other (diametric compression). The numerical and experimental failure processes of the testing samples are being illustrated in Figs. 1(a) and 1(b), respectively. These failure process shows that there is a well matching in between the numerical and laboratory testing results and the calibration process is valid. Table 2 present the tensile strength values measured experimentally with those gained numerically. Comparing these strength values shows that there is a good agreement in between the numerical and experimental results.

2.2 model preparation using particle flow code

The numerical investigation of Brazilian disc model is accomplished considering the two cases: (1) model containing a single cylindrical hole in middle and (2) specimens containing multi-holes.

2.2.1 Specimens containing a central hole (ring type disc specimens)

Some experiments have been carried out to study the mechanism of crack initiation and crack propagation in ring

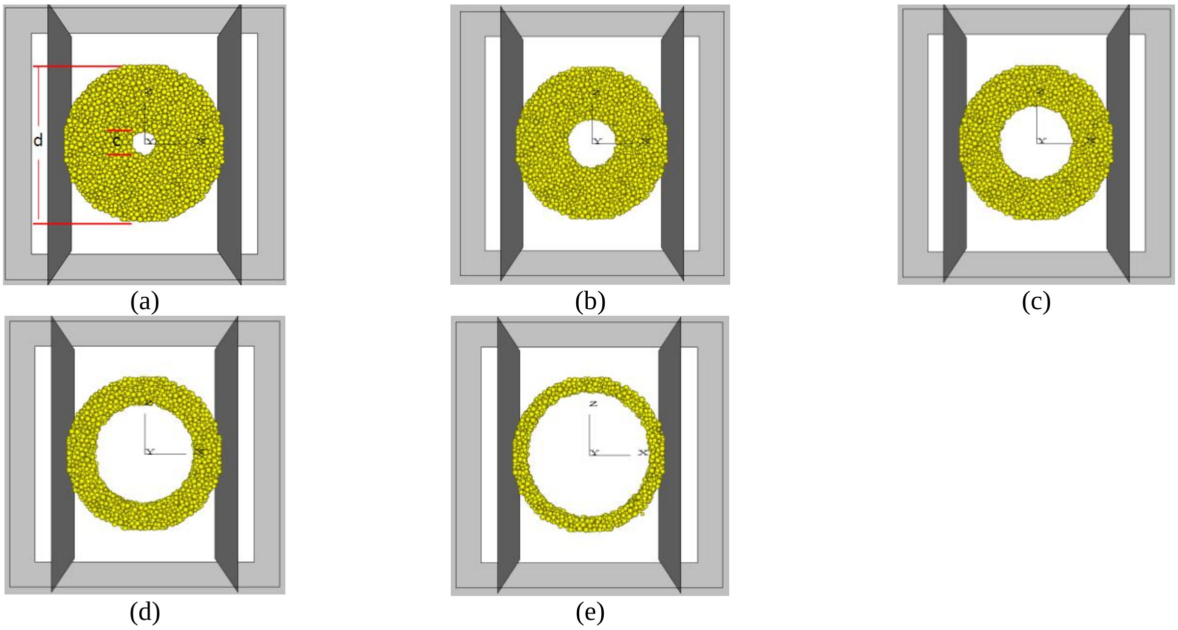

Fig. 2 Single-holed Brazilian discs under diametrical compression with different c / d ratios; (a) c / d = 0.033, (b) c / d = 0.17, (c) c / d = 0.25, (d) c / d = 0.33 and (e) c / d = 0.42

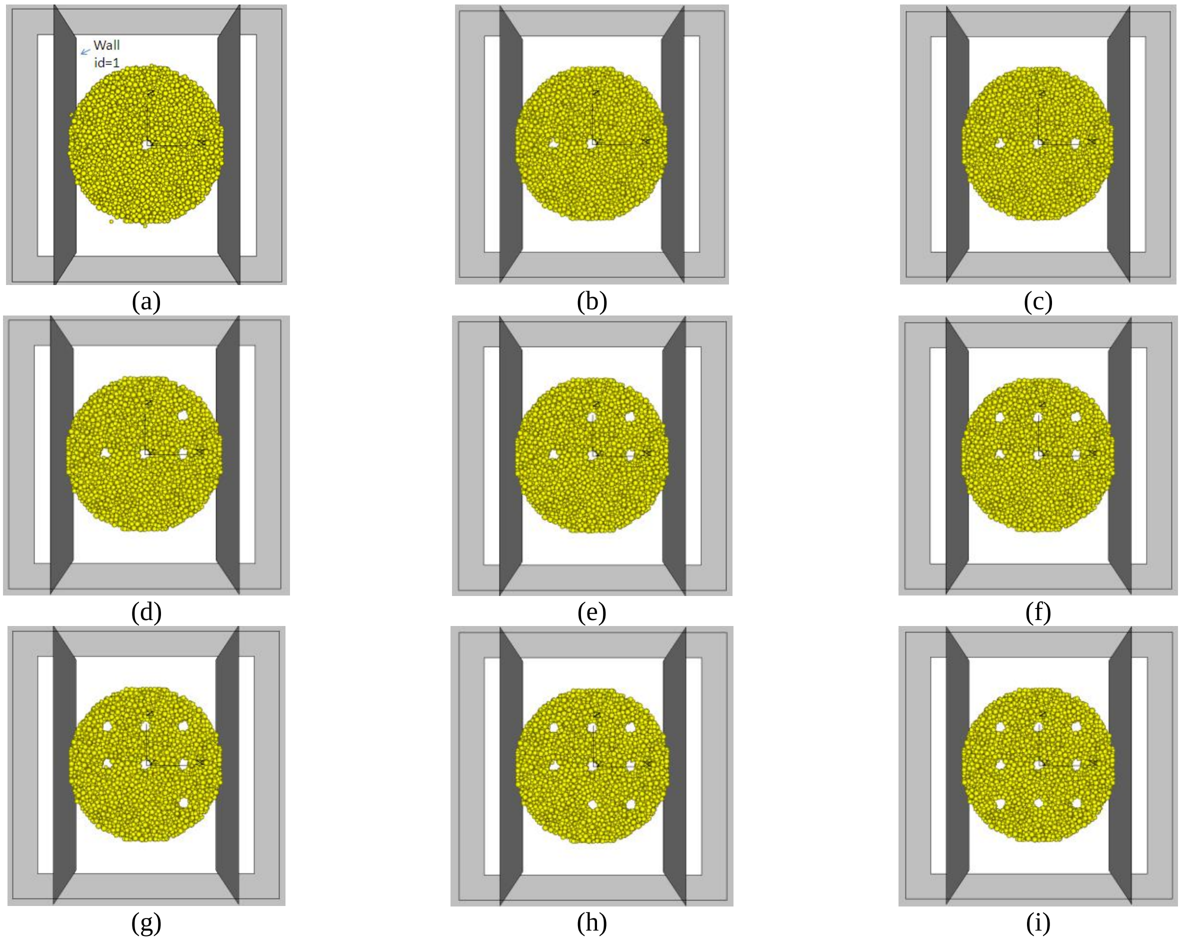

Fig. 3 disc specimens containing multi-cylindrical holes under diametrical compression; (a) one hole, (b) two hole, (c) three hole, (d) four hole, (e) five hole, (f) six hole, (g) seven hole, (h) eight hole and (i) nine hole; hole diameter was 5 mm

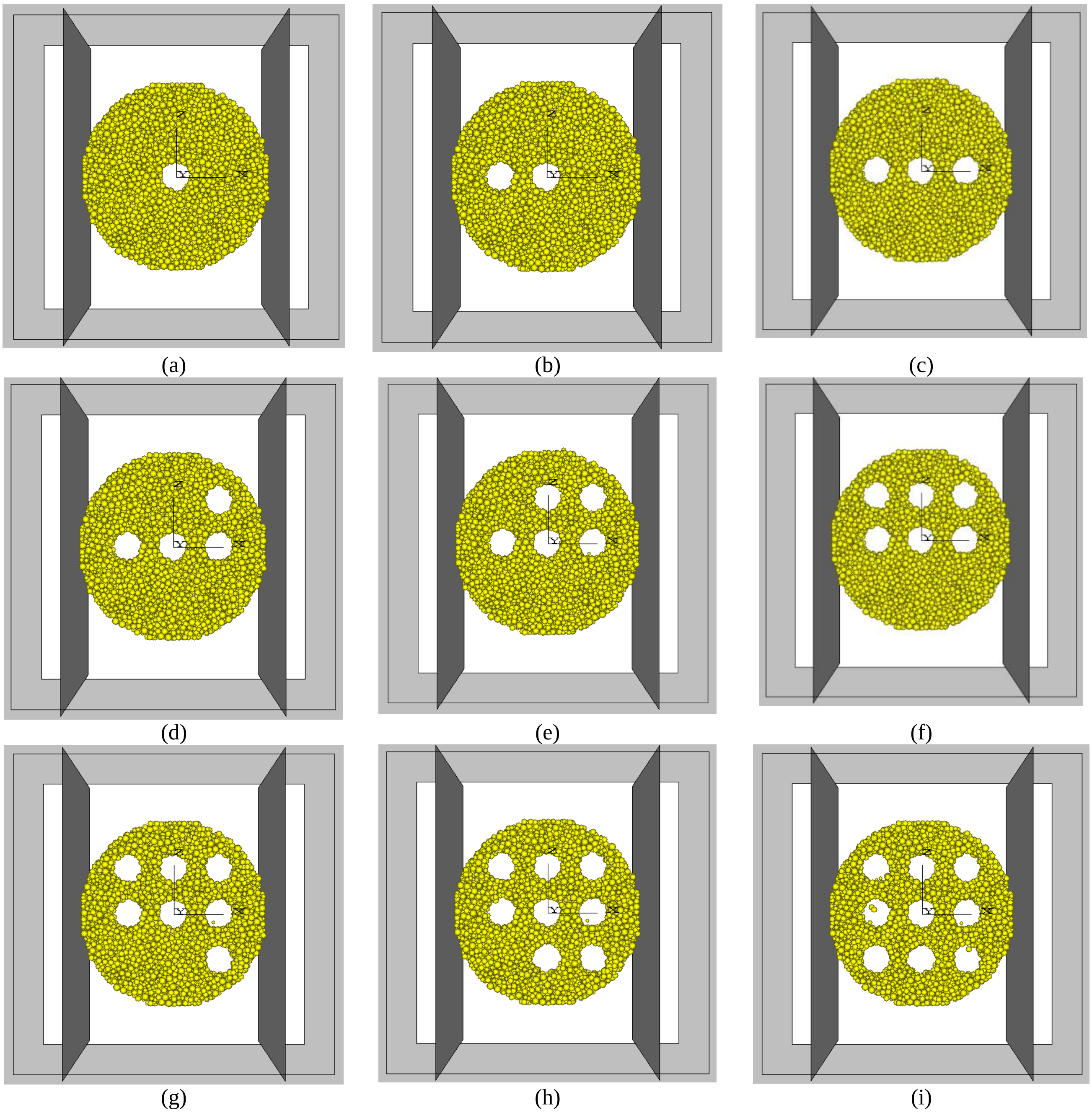

Fig. 4 Disc specimens containing multi-cylindrical holes under diametrical compression; (a) one hole, (b) two hole, (c) three hole, (d) four hole, (e) five hole, (f) six hole, (g) seven hole, (h) eight hole and (i) nine hole; hole diameter was 10 mm

type disc specimens with different c/d ratios (Fig. 2). Diameter of Brazilian model was 6 cm (d in Fig. 2) and the ratio of c/ d were 0.033, 0.17, 0.25, 0.33 and 0.42. These data were selected based on limitation in model space.

2.2.2 Brazilian discs containing multiple parallel cylindrical holes

Brazilian tensile tests were simulated by creating a circular model in PFC3D (Figs. 3-5). Nine numerical modeling have been carried out to study the mechanism of crack initiation and crack propagation in brazilian disc specimens with multiple parallel cylindrical holes (Figs. 3-5). Number of hole in models changes from 1 to 9 with increment of 1 hole. Three different diameter was used in his study; i.e., 0.5 mm (Fig. 3), 1 mm (Fig. 4) and 1.2 mm (Fig. 5). The model was crushed by lateral walls moved toward each other. The Tensile force and crack initiation force were registered by taking the reaction forces on the wall 1 in Fig. 3(a).

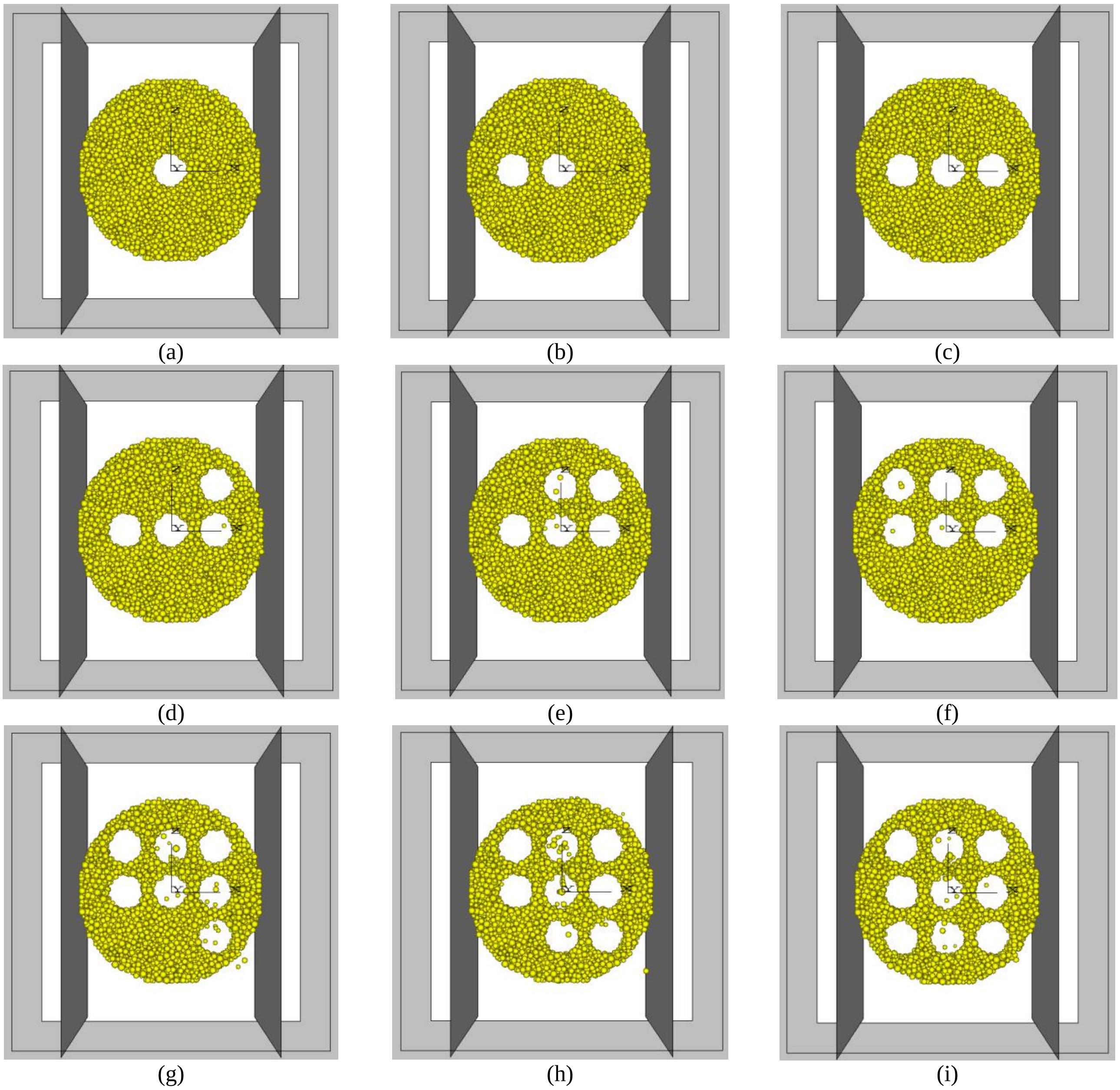

Fig. 5 Disc specimens containing multi-cylindrical holes under diametrical compression; (a) one hole, (b) two hole, (c) three hole, (d) four hole, (e) five hole, (f) six hole, (g) seven hole, (h) eight hole and (i) nine hole; hole diameter was 12 mm

3. Results

3.1 The effect of diameter of central hole on crack coalescence

When the ratio of c/ d were 0.033 (Fig. 6(a)) , it was observed that the tensile cracks initiate from right and left of model and propagate in a direction parallel to the direction of the maximum compressive stress till coalesce with the internal circle edge. In this condition several short shear bands occur in model. When ratio of c/ d were 0.17, 0.25, 0.33 and 0.42 (Figs. 6(b)-6(e)), it was observed that the tensile cracks initiate from right and left of internal hole and propagate parallel to the compressive stress till coalesce with the model boundary. In this condition single fracture surface bring model to failure. As can be observed by comparing between Fig. 6 and results rendered by Haeri *et al*. (2015), there is good accordance between numerical simulation and experimental results obtained by Haeri *et al*. (2015).

Also, the crack propagation paths shown in Fig. 6 are in good agreement with the numerical results given by Tang and Hudson (2010). Therefore, comparing the results graphically shown clearly demonstrate the accuracy and validity of the PFC3D results presented in this study. It should be noted that the PFC3D is much faster, and it is quite easy to work with it.

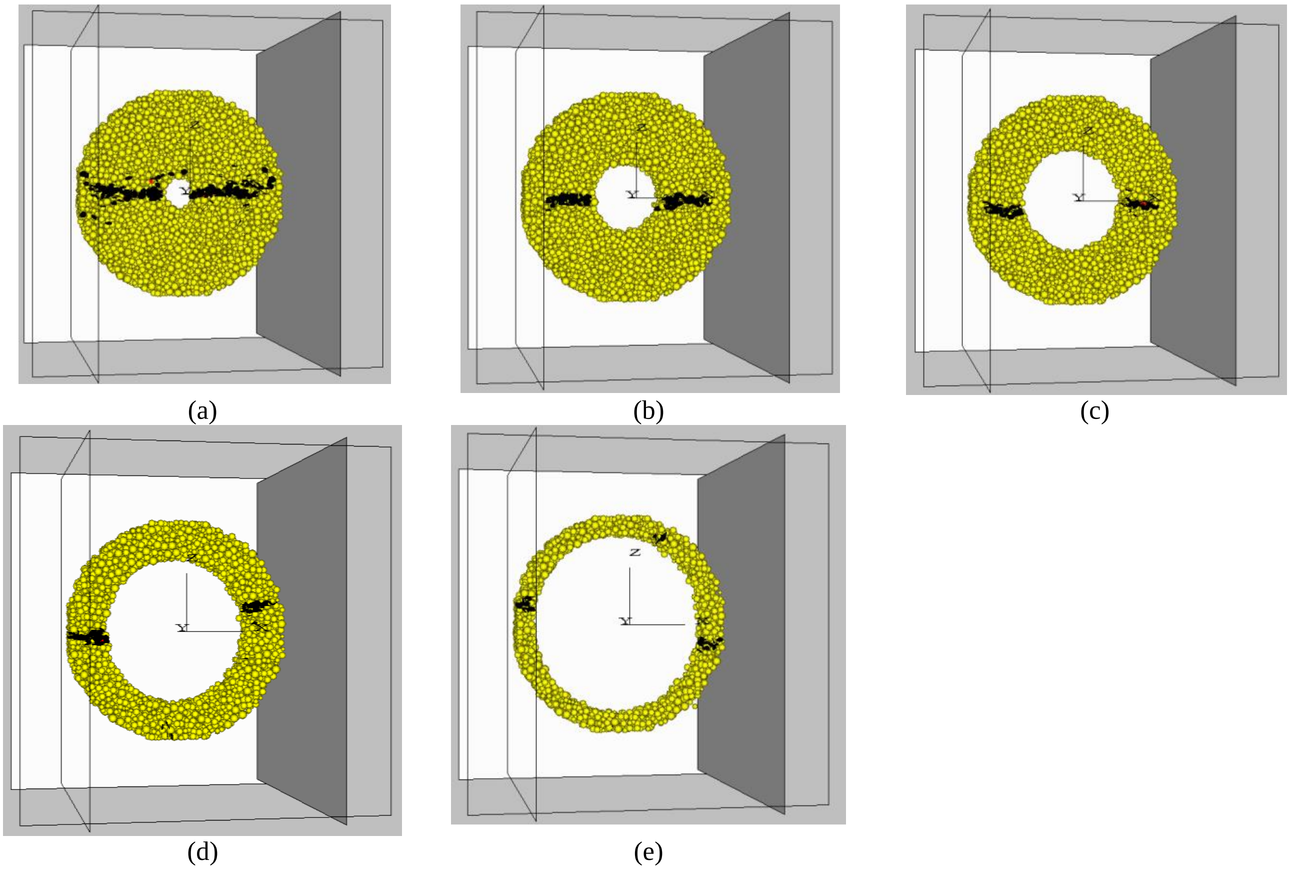

Fig. 6 numerical tests showing the cracking patterns in the single-holed Brazilian discs under diametrical compression with different c/ d ratios: (a) c /d = 0.033, (b) c /d = 0.17, (c) c/d = 0.25, (d) c/d = 0.33 and (e) c / d = 0.42

3.2 the effect of multiple parallel cylindrical holes on crack coalescence

a) Diameter of hole was 5 mm

Figs. 7(a)-7(i) shows failure pattern in numerical models. Red line and black line represent the shear crack and tensile crack, respectively. When one hole situated in the model (Fig. 7(a)), the tensile and shear cracks initiated from right and left the model and propagates toward the holes till coalesce with internal hole. In this condition hole mobilized in failure process. For the case shown in Fig. 7(b) (two holes), the tensile and shear cracks initiated from right and left the model and propagates toward the holes till coalesce with internal holes. When three hole, four hole, five hole, six hole, seven hole, eight hole and nine hole distributed in the model (Figs. 7(c)-7(i)), cracks initiate from internal holes and propagates parallel to loading direction. The specimen fails in the direction of the crack propagation paths.

b) Diameter of hole was 10 mm

Figs. 8(a)-8(i) shows failure pattern in numerical models consisting one hole, two holes, three holes, four holes, five holes, six holes, seven holes, eight holes and nine holes, respectively. Red line and black line represent the shear crack and tensile crack, respectively.

When one hole situated in the model (Fig. 8(a)), the tensile cracks initiated from right and left the model and propagates toward the holes till coalesce with internal hole. In his condition hole mobilized in failure process. For the case shown in Fig. 8(b) (two holes), the tensile cracks initiated from right and left the model and propagates toward the holes till coalesce with internal holes.

When three hole, four hole, five hole and six hole distributed in the model (Figs. 8(c)-(f)), tensile cracks initiate from internal holes and propagates parallel to loading direction. The specimen fails in the direction of the crack propagation paths i.e., only three crack mobilized in failure process.

When seven holes, eight holes and nine holes distributed in the model (Figs. 8(g)-8(i)), tensile cracks initiate from four holes and propagate parallel to loading direction. The specimen fails in the direction of the crack propagation paths.

c) Diameter of hole was 12 mm

Figs. 9(a)-9(i) shows failure pattern in numerical models consisting one hole, two holes, three holes, four holes, five holes, six holes, seven holes, eight holes and nine holes, respectively. Red line and black line represent the shear crack and tensile crack, respectively.

When one hole situated in the model (Fig. 9(a)), the tensile cracks initiated from right and left the model and propagates toward the holes till coalesce with internal hole. In his condition hole mobilized in failure process. For the case shown in Fig. 9b and c (two holes and three holes), the tensile cracks initiated from right and left the model and propagates toward the holes till coalesce with internal holes.

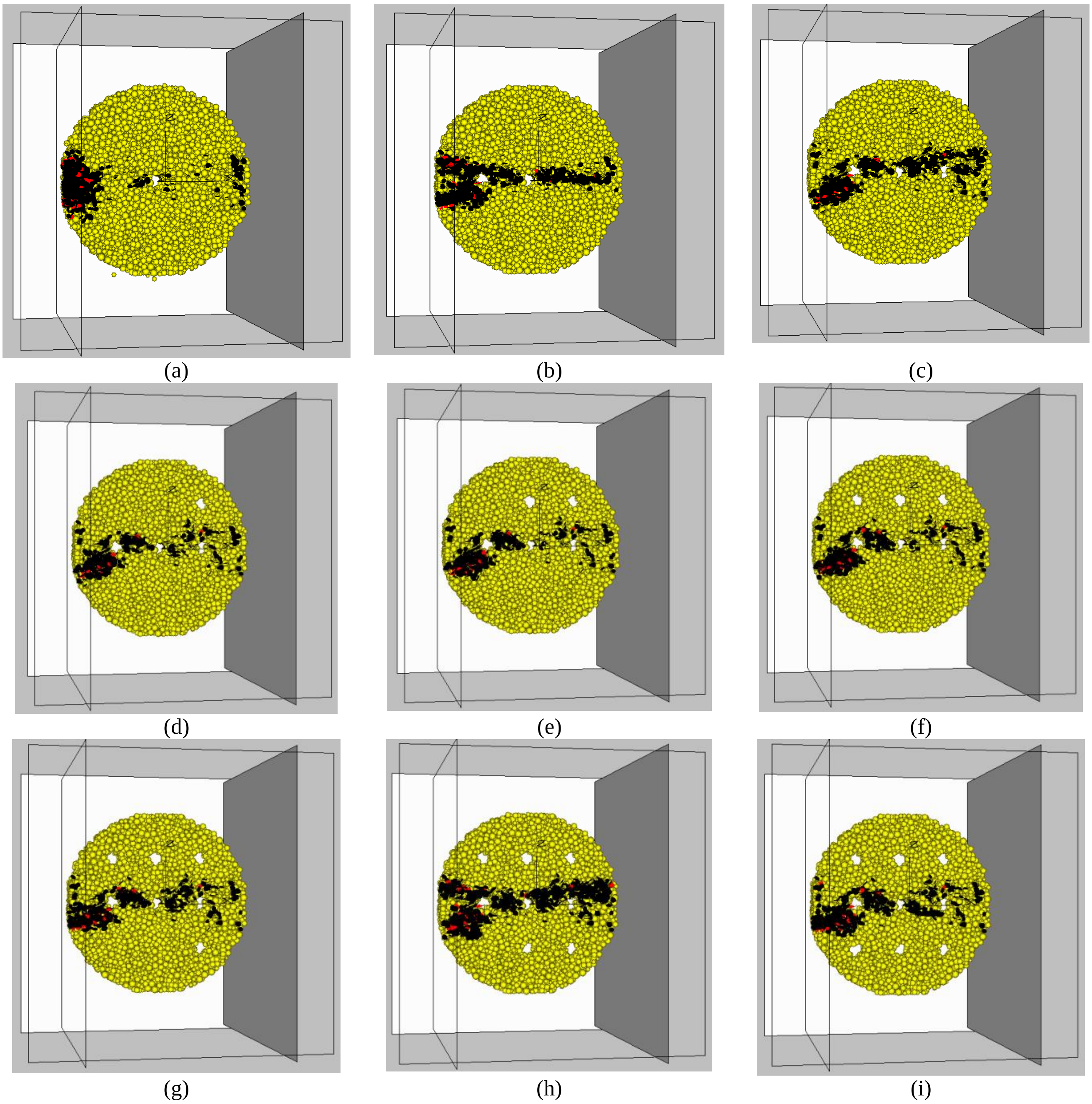

Fig. 7 Failure pattern in numerical models consisting (a) one hole, (b) two holes, (c) three holes, (d) four holes, (e) five holes, (f) six holes, (g) seven holes, (h) eight holes and (i) nine holes; hole diameter was 5mm

When four hole, five hole and six hole distributed in the model (Figs. 9(d)-9(f)), tensile cracks initiate from four holes and propagates parallel to loading direction. The specimen fails in the direction of the crack propagation paths i.e., only three cracks mobilized in failure process.

When seven holes, eight holes and nine holes distributed in the model (Figs. 9(g)-9(i)), tensile cracks initiate from six holes and propagate parallel to loading direction. The specimen fails in the direction of the crack propagation paths.

As can be observed by comparing between Figs. 7(c), 8(c) and 9(c) and Fig. 10(a), there is good accordance between numerical simulation and experimental results obtained by Haeri *et al.* (2015).

Haeri *et al*. (2015) simulate numerically crack propagation in Brazilian disc with same internal hole configuration. Comparison between Figs. 7(c), 8(c) and 9(c) and Fig. 10(b), shows that the simulated propagation paths are in good agreement with the corresponding high order DDM numerical results obtained by Haeri *et al.* (2015).

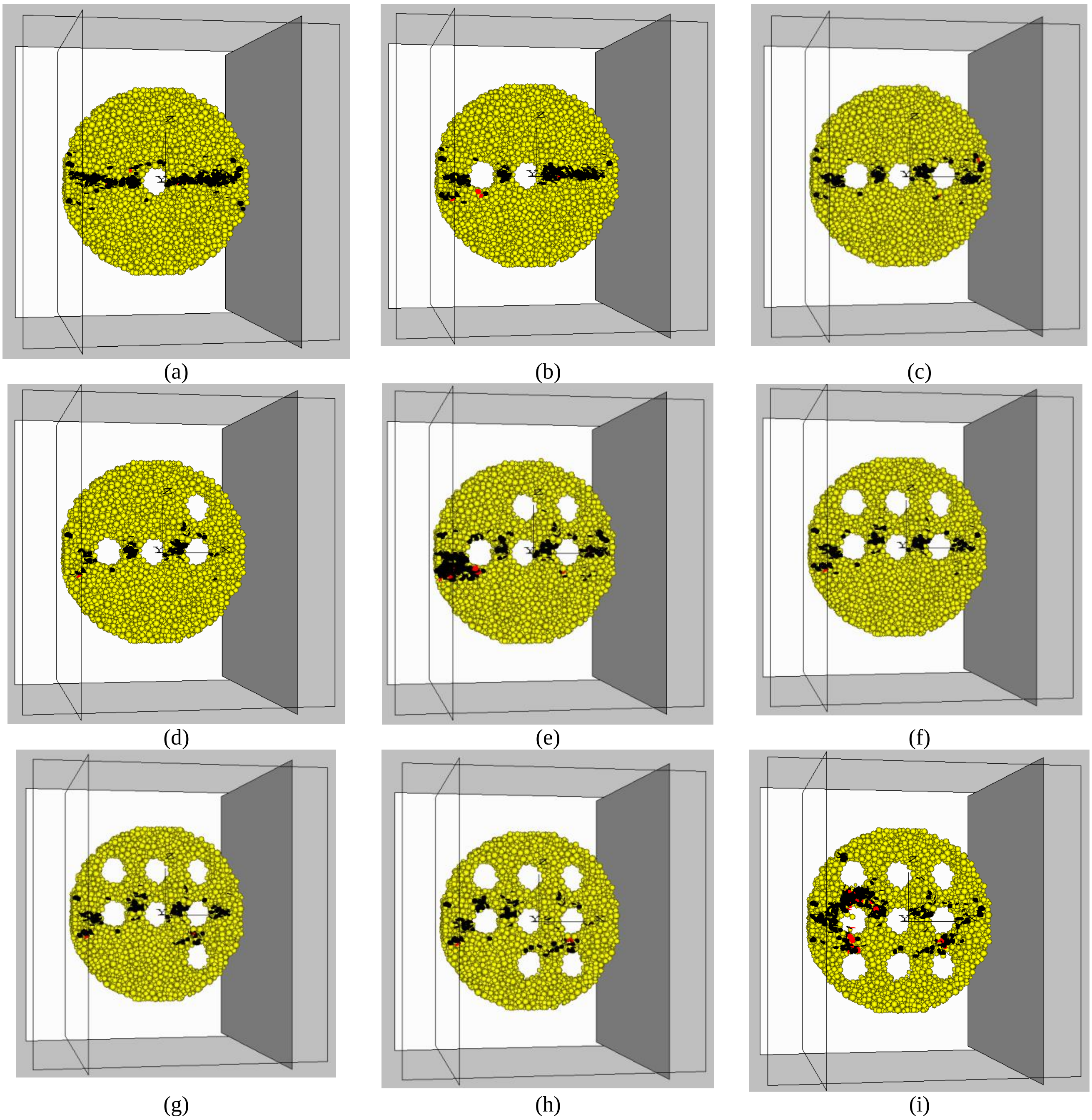

Fig. 8 failure pattern in numerical models consisting (a) one hole, (b) two holes, (c) three holes, (d) four holes, (e) five holes, (f) six holes, (g) seven holes, (h) eight holes and (i) nine holes; hole diameter was 10 mm

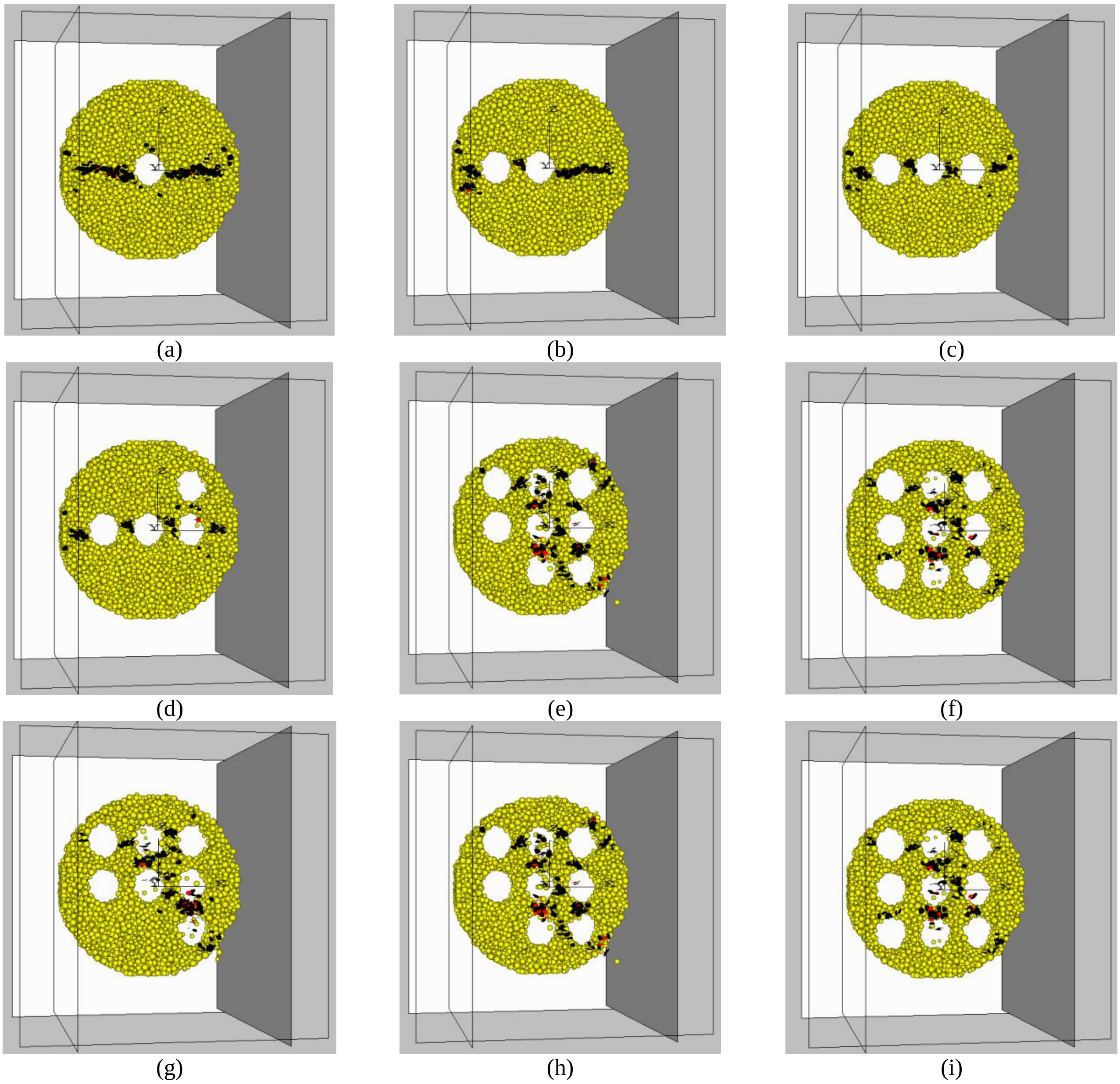

Fig. 9 failure pattern in numerical models consisting (a) one hole, (b) two holes, (c) three holes, (d) four holes, (e) five holes, (f) six holes, (g) seven holes, (h) eight holes and (i) nine holes; hole diameter was 12 mm

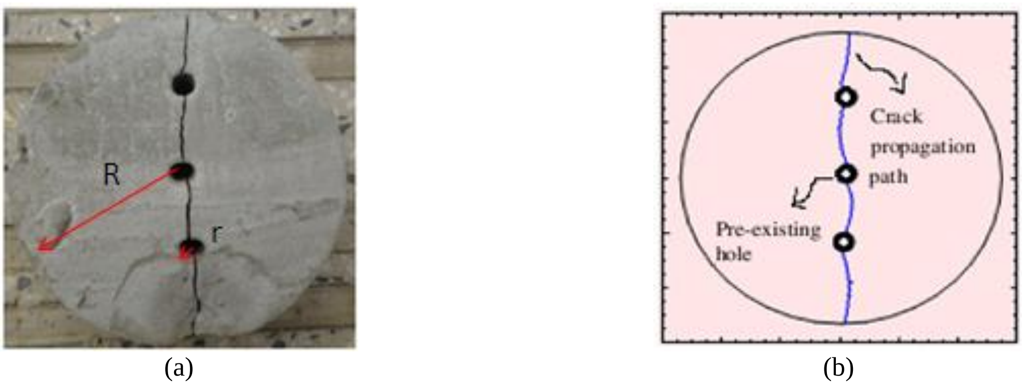

Fig. 10 The cracking patterns in the disc specimens containing multi-cylindrical holes (r/R = 0.006) under diametrical compression. (a) Vertical arrangements of three holes in disc specimens and (b) Vertical arrangements of three holes in disc model (Haeri *et al*. 2015)

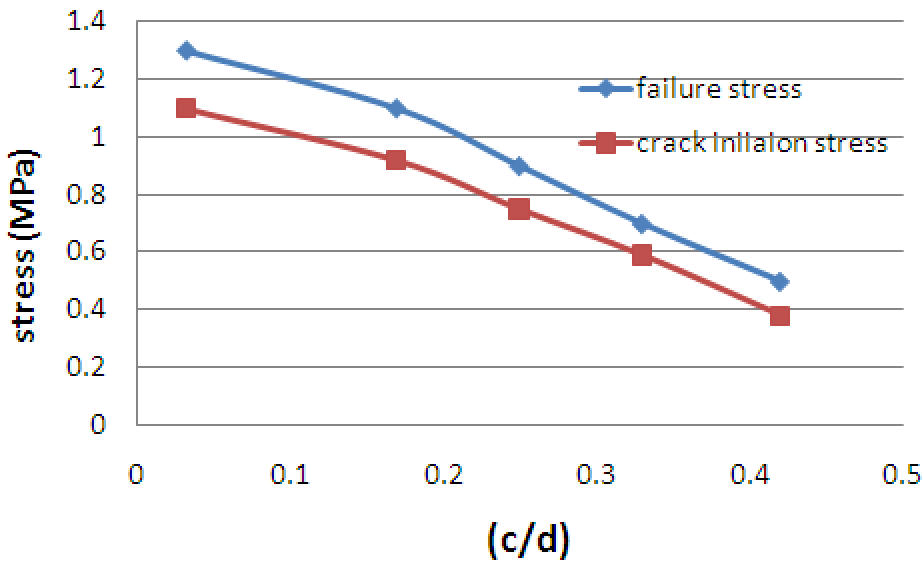

Fig. 11 The effect of hole diameter on the failure stresses and crack initiation stress

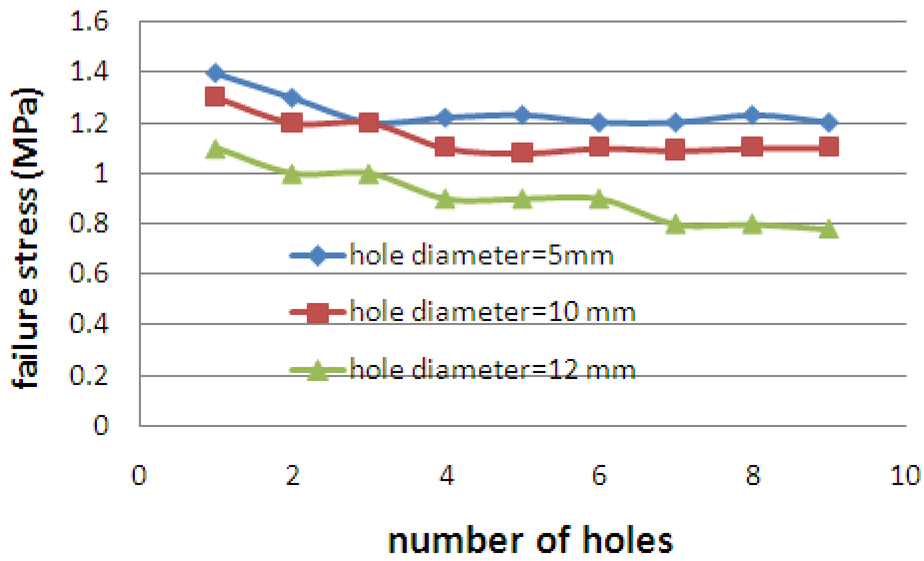

Fig. 12 The effect of number of hole on the failure stresses of model

3.3 The effect of internal hole diameter on the failure stress

Fig. 11 shows the effect of hole diameter on the failure stresses and crack initiation stress. The failure stress and crack initiation stress decreases by increasing the hole diameter.

Fig. 12 shows the effect of number of hole on the failure stresses of model. The failure stress decreases by increasing the number of hole which mobilized in failure. When hole diameter was 5mm, the failure stress decrease till the number of holes were three. By increasing the hole more than three, the failure stress was fixed. When hole diameter was 10mm, the failure stress decrease till the number of holes were four. By increasing the hole more than four, the failure stress was fixed. When hole diameter was 12 mm, the failure stress decrease till the number of holes were seven. By increasing the hole more than seven, the failure stress was fixed.

4. Conclusions

The subject of cracks propagation and cracks coalescence in brittle solids such as rock and concrete has gotten much attention in recent years. Further research may be devoted to investigating the mechanism of the crack propagation process in rocks and rock-like materials. In this research, effects of the breaking load in Brazilian disc concrete models each containing a single hole of different size is studied first. The failure stress and failure pattern analyses are accomplished numerically and the results are compared and discussed. Then, some pre-holed Brazilian discs are tested under compression and the numerical results are compared with the numerically simulated results obtained by using the higher order displacement discontinuity method (a version of the indirect boundary element method). It is concluded that:

- The crack propagation mechanism in the brittle solids such as rocks and concrete may occur due to the cracks coalescence phenomenon in the bridge area, which is mainly caused by propagation of tensile radial cracks emanating from the surface of the central holes.
- It has been observed that the corresponding numerical results are in good agreement with the experimental and numerical results rendered by other researchers.
- Comparing the PFC numerical results with DDM results illustrates that the tensile cracks and the cracks propagation paths are mainly produced by the coalescence phenomenon of the preexisting multi-holes in models.
- Based on the present analyses, it may be also concluded that the cracks may be initiated radially near the surface of the holes, the stress concentration can be released and finally, stresses in the specimen can redistributed to attain a new equilibrium condition. Then, the final breaking of the pre-holed disc specimens may be due to the propagation of radially induced tensile cracks initiated from the surface of the central hole and propagating toward the direction of diametrical loading and/or perpendicular to it (for the case of specimens with larger holes).
- In the case of disc specimens with multiple holes, the cracks propagation and cracks coalescence may occur simultaneously in the breaking process of model under diametrical compressive loading.
- The failure stress and crack initiation stress decreases by increasing the hole diameter.
- The failure stress decreases by increasing the number of hole which mobilized in failure. When pore diameter was 5 mm, both of the tensile and shear cracks bring model to failure. By increasing the hole diameter only tensile crack induced in the model.

References

Akbas, S, (2016), "Analytical solutions for static bending of edge cracked micro beams", *Struct. Eng. Mech*., **59**(3), 66-78.

Aliabadi, M.H. and Brebbia, C.A. (1993), Advances in Boundary Element Methods for Fracture Mechanics. Amsterdam: Elsevier.

Al-Shayea, N.A. (2005), "Crack propagation trajectories for rocks under mixed mode I–II fracture", *Eng. Geol*., **81**, 84-97.

Amadei, B., Lin, C. and Jerry, D. (1996), Recent extensions to the DDA method. In: Proceedings of the First International Forum on Discontinuous Deformation Analysis (DDA) and Simulations of Discontinuous Media.Albuquerque: TSI Press. p. 1-3.

Ashby, M.F. and Hallam, S.D. (1986), "The failure of brittle solids containing small cracks under compressive stress states", *Acta Metal*., **34**(3), 497-510.

Cundall, P.A. and Strack, O.D.L. (1979), "A discrete numerical model for granular assemblies", *Geotechnique*, **29**(1), 47-65.

Fan, Y., Zhu, Z., Kang, J. and Fu, Y. (2016), "The mutual effects between two unequal collinear cracks under compression", *Math. Mech. Solids*, **22**,1205-1218.

Gerges, N., Issa, C. and Fawaz, S. (2015), "Effect of construction joints on the splitting tensile strength of concrete", *Case Studies Constr. Mater*., **3**, 83-91.

Ghazvinian, A., Sarfarazi, V., Schubert, W. and Blumel, M. (2012), "A study of the failure mechanism of planar non-persistent open joints using PFC2D", *Rock Mech. Rock Eng*., **45**(5), 677-693,

Haeri, H., Sarfarazi, V., Fatehi, M., Hedayat, A. and Zhu, Z. (2016c), "Experimental and numerical study of shear fracture in brittle materials with interference of initial double", *Acta Mech. Soil. Sinic*., **5**, 555-566.

Haeri, H., Khaloo, A. and Marji, M.F. (2015a), "Experimental and numerical simulation of the microcrack coalescence mechanism in rock-like materials", *Strength Mater*., **47**(5), 740-754.

Haeri, H., Khaloo, A. and Marji, M.F. (2015b), "Fracture analyses of different pre-holed concrete specimens under compression", *Acta Mech. Sinic*., **31**(6), 855-870.

Haeri, H., Khaloo, A. and Marji, M.F. (2015c), "A coupled experimental and numerical simulation of rock slope joints behavior", *Arab. J. Geosci*., **8**(9), 7297-7308.

Haeri, H., Sarfarazi, V. and Hedayat, A. (2016a), "Suggesting a new testing device for determination of tensile strength of concrete", *Struct. Eng. Mech*., **60**(6), 939-952.

Haeri, H., Sarfarazi, V. and Lazemi, H. (2016b), "Experimental study of shear behavior of planar non-persistent joint", *Comput. Concrete*, **17**(5), 639-653.

Haeri, H. and Sarfarazi, V. (2016), "The effect of non-persistent joints on sliding direction of rock slopes", *Comput. Concrete*, **17**(6), 723-737.

He, L. and Ma, G.W. (2010), "Development of 3D numerical manifold method", *Int. J. Comput. Meth*., **7**(1)107-129.

Jespersen, C., Maclaughlin, M. and Hudyma, N. (2010), "Strength deformation modulus and failure modes of cubic analog specimens representing macroporus rock", *Int. J. Rock Mech. Min. Sci*., **47**, 1349-1356.

Kequan, Y.U. and Zhoudao, L.U. (2015), "Influence of softening curves on the residual fracture toughness of post-fire normal-strength mortar", *Comput. Mortar*, **15**(2), 102-111.

Lajtai, E.Z. and Lajtai, V.N. (1975), "The collapse of cavities", *Int. J. Rock Mech. Min. Sci. Geomech. Abstr*., **12**, 81-86.

Lancaster, I.M., Khalid, H.A. and Kougioumtzoglou, I.A. (2013), "Extended FEM modelling of crack propagation using the semi-circular bending test", *Constr. Build. Mater*., **48**, 270-277

Lee, S. and Chang, Y. (2015), "Evaluation of RPV according to alternative fracture toughness requirements", *Struct. Eng. Mech*., **53**(6), 1271-1286.

Li, S., Wang, H., Li, Y., Li, Q., Zhang, B. and Zhu, H. (2016), "A new mini-grating absolute displacement measuring system for static and dynamic geomechanical model tests", *Measurement*, **82**, 421-431.

Li, Y., Zhou, H., Zhu, W., Li, S. and Liu, J. (2015), "Numerical study on crack propagation in brittle jointed rock mass influenced by fracture water pressure", *Materials*, **8**(6), 3364-3376.

Lin, P., Ma, T.H., Liang, Z.Z., Tang, C.A. and Wang, R.K. (2014), "Failure and overall stability analysis on high arch dam based on DFPA code", *Eng. Fail. Anal*., **45**, 164-184.

Lin, P., Wang, R.K., Wong, R.H.C. and Zhou, W.Y. (2005), "Crack coalescence mechanism of brittle solids containing holes under uniaxial compression", *Proceedings of the EuRock 2005*, London.

Lin, P., Wong, R.H.C. and Tang, C.A. (2015), "Experimental study of coalescence mechanisms and failure under uniaxial compression of granite containing multiple holes", *Int. J. Rock Mech. Min. Sci.*, **77**, 313-327.

Lin, P., Zhou, Y.N., Liu, H.Y. and Wang, C. (2013), "Reinforcement design and stability analysis for large-span tailrace bifurcated tunnels with irregular geometry", *Tunn. Undergr. Sp. Tech*., **38**(9), 189-204.

Mellor, M. and Hawkes, I. (1971), "Mesurment of tensile strength by diametral compression on disc and annuli", *Eng. Geol*., **5**, 173-225.

Mobasher, B., Bakhshi, M. and Barsby, C. (2014), "Backcalculation of residual tensile strength of regular and high performance fibre reinforced concrete from flexural tests", *Constr. Build. Mater*., **70**, 243-253.

Mohammad, A. (2016), "Statistical flexural toughness modeling of ultra-high performance mortar using response surface method", *Comput. Mortar*, **17**(4), 33-39.

Nemat-Nasser, S. and Horii, H. (1982), "Compression-induced nonlinear crack extension with application to splitting, exfoliation, and rockburst", *J. Geophys. Res*., **87**(8), 6805-6821.

Noel, M. and Soudki, K. (2014), "Estimation of the crack width and deformation of FRP-reinforced concrete flexural members with and without transverse shear reinforcement", *Eng. Struct*., **59**, 393-398.

Oliveira, H.L. and Leonel, E.D. (2014), "An alternative BEM formulation, based on dipoles of stresses and tangent operator technique, applied to cohesive crack growth modeling", *Eng. Anal. Bound. Elem*., **41**, 74-82.

Pan, B., Gao, Y. and Zhong, Y. (2014), "Theoretical analysis of overlay resisting crack propagation in old cement mortar pavement", *Struct. Eng. Mech*., **52**(4) 167-181.

Park, C.H. and Bobet, A. (2009), "Crack coalescence in specimens with open and closed flaws :a comparison", *Int. J. Rock Mech. Min. Sci*., **46**, 819-829.

Rajabi, M., Soltani, N. and Eshraghi, I. (2016), "Effects of temperature dependent material properties on mixed mode crack tip parameters of functionally graded materials", *Struct. Eng. Mech*., **58**(2), 144-156.

Ramadoss, P. and Nagamani, K. (2013), "Stress-strain behavior and toughness of high performance steel fiber reinforced mortar in compression", *Comput. Mortar*, **11**(2), 55-65.

Robert, L.K. (1979), "Crack– crack and crack– hole interactions in stressed granite", *Int. J. Rock Mech. Min. Sci*., **16**, 37-47.

Roy, Y.A. and Narasimhan, R.A. (1999), "Finite element investigation of the effect of crack tip constraint on hole growth under mode I and mixed mode loading", *Int. J. Solids Struct*., **36**, 1427-1447.

Sammis, C.G. and Ashby, M.F. (1986), "The failure of brittle porous solids under compressive stress states", *Acta Metal*., **34**, 511-526.

Sammis, C.G. and Ashby, M.F. (1986), "The failure of brittle porous solids under compressive stress states", *Acta. Metal.*, **34**, 511-526.

Sardemir, M. (2016), "Empirical modeling of flexural and splitting tensile strengths of concrete containing fly ash by GEP", *Comput. Concrete*, **17**(4), 489-498.

Sarfarazi, V., Ghazvinian, A., Schubert, W., Blumel, M. and Nejati, H.R. (2014), "Numerical simulation of the process of fracture of echelon rock joints", *Rock Mech. Rock Eng*., **47**(4), 1355-1371.

Sarfarazi, V., Haeri, H. and khaloo, A. (2016a), "The effect of non-persistent joints on sliding direction if rock slopes", *Comput. Concerete*, **7**, 723-737.

Shi, G.H. (1988), Discontinuous Deformation Analysis, a New Numerical Mode l for the Statics and Dynamics of Block System. Berkeley: Department of Civil Engineering, University of California; 1988 [Ph.D. dissertation].

Shuraim, A.B., Aslam, F., Hussain, R. and Alhozaimy, A. (2016), "Analysis of punching shear in high strength RC panels– experiments, comparison with codes and FEM results", *Comput. Concrete*, **17**(6), 33-49.

Silva, R.V., Brito, J. and Dhir, R.K. (2015), "Tensil strength behaviour of recycled aggregate concrete", *Constr. Build. Mater*., **83**, 108-118.

Sukumar, N.A. and Prevost, J.H. (2003), "Modeling quasi-static crack growth with the ex-tended finite element method, Part I: Computer implementation", *Int. J. Solids Struct.*, **40**, 7513-7537.

Tan, X.C., Kou, S.Q. and Lindqvist, P.A. (1998), "Application of the DDM and fracture mechanics model on the simulation of rock breakage by mechanical tools", *Eng. Geol*., **3-4**, 277-284.

Tang, C.A. and Hudson, J.A. (2010), Rock failure mechanisms: illustrated and explained. CRC Press, Boca Raton.

Tiang, Y., Shi, S., Jia, K. and Hu, S. (2015), "Mechanical and dynamic properties of high strength concrete modified with lightweight aggregates presaturated polymer emulsion", *Constr. Build. Mater*., **93**, 1151-1156.

Wan Ibrahim, M.H., Hamzah, A.F., Jamaluddin, N,, Ramadhansyah, P.J. and Fadzil, A.M. (2015), Split Tensile Strength on Self-compacting Concrete Containing Coal Bottom Ash, Procedia - Social and Behavioral Sciences, **198**, 2280-2289.

Wang, X., Zhu, Z., Wang, M., Ying, P., Zhou, L. and Dong, Y. (2017), "Study of rock dynamic fracture toughness by using VB-SCSC specimens under mediumlow speed impacts", *Eng. Fract. Mech*., **181**, 52-64.

Wong, R.H.C. and Chau, K.T. (1998), "Crack coalescence in rock-like material containing two cracks", *Int. J. Rock Mech. Min. Sci*., **35**(2), 147-164 .

Yaylac, M. (2016), "The investigation crack problem through numerical analysis", *Struct. Eng. Mech*., **57**(6), 55-68.

Yin, P. (2013), Multiple Surface Crack Coalescence Mechanisms in Granite.The Hong Kong Polytechnic University; [Ph.D. thesis].

Zheng, H. (2009), "Discontinuous deformation analysis based on complementary theory", *Sci. China Ser. E. Tech. Sci*., **52**(9), 2547-2554.

CC